Estimation of Suspended Particulate Matter Using Landsat 9 Imagery: Generating Algorithms and Spatio-Temporal Distributions

Lilik Maslukah[1]*, M. Firouz Dimas Sadewo[2], Baskoro Rochaddi[1], Sugeng Widada[1], Anindya Wirasatriya[1], Ulung Jantama Wisha[3,4]

[1]Department of Oceanography, Faculty of Fisheries and Marine Sciences, Universitas Diponegoro
[2]Undergraduate Program of Oceanography, Faculty of Fisheries and Marine Science, Universitas Diponegoro
Jl. Prof. Jacub Rais, Tembalang Semarang Central Java, 50275 Indonesia
[3]Physical Oceanography Laboratory, Faculty of Science, University of the Ryukyus, Nishihara, Japan
[4]Coastal Processes Research Group, Research Center for Oceanography, National Research and Innovation Agency Jakarta, Indonesia
Email: lilik_masluka@yahoo.com

Abstract

The fluctuation of suspended particulate matter (SPM) is essential to the biogeochemical cycle and ecological health of coastal waters. Anthropogenic activities potentially trigger an increase in SPM, so it needs to be monitored continuously. Spatial and temporal monitoring of SPM can be carried out cost-effectively with broad coverage using a remote sensing application. This study aims to build the SPM algorithm and estimate its temporal variability. The algorithm model in this study is based on an empirical formula between field data and reflectance data with the same acquisition. Water samples were taken from 100 stations in July 2022. Half were used for model building and the other for model validation. Suspended Particulate Matter was determined gravimetrically and estimated their temporal variability was based on Landsat 9 image records from December 2021 - November 2022. The results of the analysis show that the best algorithm for SPM estimation can be built based on coastal aerosol canals (B1), blue canals (B2), and green canals (B3) with the accuracy test result of (R^2 = 0.68; RMSE = 5.551 $mg.L^{-1}$; MAPE= 7.07%; Bias= 0.28). The SPM temporal fluctuations were generally higher in the west monsoon and lowered in the east monsoon, ranging from 30 to 70 $mg.L^{-1}$. On the other hand, the spatial distribution shows a higher magnitude in the estuary than in the offshore waters, with a deviation of about 30 $mg.L^{-1}$. Regional authorities can use the results obtained to improve the management of coastal water quality and monitoring systems.

Keywords: *Algorithm, Spatial analysis, Landsat 9, Banjir Kanal Timur*

Introduction

Human activities on land have greatly affected coastal waters. Although they constitute a small portion of the total global ocean, these coastal waters are ecologically, socially, and economically important. They supply up to 90% of global fish yields (Colella *et al*., 2016). Coastal waters are susceptible to getting degraded due to anthropogenic-sourced pollutions that potentially deteriorate water quality and cause undesirable effects, such as an increase in turbidity, sediment silting, and even eutrophication. Banjir Kanal Timur (BKT) estuary is a flood control system of Semarang City located in the eastern part of the city. The length of this river is about 14.50 km. The Banjir Kanal Timur River flows from the Penggaron River through the Pucanggading Outlet Gate, Kedung Mundu River Drainage Outlet, Candi River, Bajak River, Kartini Pump Drainage, Sambirejo Pump Drainage and ends in the Java Sea. The estuary becomes turbid during the rainy season because of the high rate of sediment from the mainland in the marine waters (Wirasatriya *et al*., 2023).

The suspension concentration in the water column is often referred to as TSS ($g.m^{-3}$ or $mg.L^{-1}$) or suspended particulate matter (SPM). The suspended material consists of living organic particulates (i.e. phytoplankton, bacteria, fungi) and non-living (detrital) particulates such as clay and other minerals suspended in the water column. These suspended sediments, consisting of organic and inorganic particles, originate from natural processes or are the result of human activities on land and coastal waters (Balasubramanian *et al*., 2020; Niroumand-Jadidi *et al*., 2022). The flow of river water from land is the main contribution of suspended material in estuarine waters (Irwansyah *et al.,* 2023; Wirasatriya *et al*., 2023). Hutasuhut *et al*. (2022) also explained that the resuspension process by tidal currents causes the suspended material in the water column to fluctuate. In addition, dredging activities are also one source of increased SPM.

*) Corresponding author

https://ejournal.undip.ac.id/index.php/ijms
DOI: 10.14710/ik.ijms.29.1.15-28
Received : 09-11-2023
Accepted : 16-01-2024

High sediment inputs to the aquatic environment can have a negative impact on water quality. It has the potential to increase temperatures in the upper layers of the water column (Wang *et al*., 2017), carrying nutrients that affect eutrophication (Wang *et al*., 2017; Maslukah *et al*., 2020; Cai *et al*., 2022; Balasubramanian *et al*., 2020; Adjovu *et al*., 2023). The high level of SPM also has an optical effect, reducing the penetration of light into deeper layers and affecting benthic organisms, reducing primary productivity so that ecosystem functions are disturbed. In the same way, sediment is critical in maintaining accretion rates and protecting the coastal geomorphic features and mangrove wetlands. These geomorphic features support and protect the blue carbon of coastal wetlands and are essential defenses against storm surges and flooding events resulting from high spring tides (Weston, 2014). Therefore, the monitoring of suspended sediments is essential in the sustainable management of ecosystems in coastal waters (Wang *et al*., 2017; Adjovu *et al*., 2023). The estuary of a river is partly enclosed water where freshwater flowing into the river mixes with saltwater as influenced by tides and waves. During the processes of water flow from the mainland to the sea and vice versa, SPM transports are possible.

Suspended sediment monitoring is usually carried out by conventional methods through sampling and analysis in the laboratory. The spatial and temporal distribution of SPM in the inshore column is very dynamic, therefore monitoring through sampling in the field is often considered inadequate (Doxaran *et al*., 2012; Adjovu *et al*., 2023). Monitoring the presence of SPM, as a parameter of water quality, can be carried out using a remote sensing (Rs) approach. This method can be applied to inland waters, lakes, estuaries, and the open sea. Mishra *et al*. (2013) and Sahoo *et al*. (2022) have proven the efficiency of using RS in characterizing the optical and bio-optical properties of water in monitoring water quality parameters such as TSS, turbidity, and chlorophyll concentration. Several satellite remote sensing products that are often used in monitoring water quality parameters are Moderate Resolution Imaging Spectroradiometer (MODIS), Landsat, SeaWiFS, and Medium Resolution Imaging Spectrometer (MERIS). Remote sensing, which works based on the optical properties reflected by the water surface, is an efficient proxy for monitoring at local, regional, and global scales (Nechad *et al*., 2009; Feng *et al*., 2014; Saberioona *et al*., 2020; Adjovu *et al*., 2023).

Reflectance remote sensing (Rrs) is one of the main products of aquatic color remote sensing. It represents the ratio of radiance leaving the water and is related to the reflectance of water (ρw) (Balasubramanian, 2020), which can be quantified from satellite sensor observations through the atmospheric effect elimination of the prior acquisition (from the top of the atmosphere (TOA) reflectance measurements) (Gordon and Wang, 1994). The presence of SPM in the water has inherent optical properties (IOP) that can be determined from the Rrs product. Previous research has developed several satellite sensor algorithms that can transform reflectance values (Rrs) so that the coastal water's quality parameters and their dynamics can be estimated (Saberioona *et al*., 2020; Shaik *et al*., 2021). In this monitoring, especially for narrow areas such as estuaries or coastal waters, high-resolution satellites will be required.

The concentration of near-surface SPM can be obtained from analytical, empirical, and semi-empirical relationships. These model relationships use Rrs(λ) of a single or the combination of multiple wavelengths (bands) (Zhang *et al*., 2014; Saberioona *et al*., 2020; Ouma *et al*., 2020; Wirasatriya *et al*., 2023). The analytical model-based analysis approach is used to solve the radiative transfer equation to estimate optically active constituents, such as SPM (Bernardo *et al*., 2019; Sagan *et al*., 2020). The application of the radiative transfer equation is derived from the outflowing radiance of the water. Zheng and DiGiacomo, (2017) have shown the inaccuracy of the inversion model (analytical model) in estimating high turbidity levels in coastal areas. The estimates of TSS developed for areas affected significantly by phytoplankton are different from those without the presence of phytoplankton (Balasubramanian *et al*., 2020). Therefore, an empirical model was developed to resolve this problem. This empirical model was developed based on the statistical relationship between in situ SPM observations and band reflectance derived by satellite sensors. Empirical models can be implemented more effectively and easily (Yu *et al*., 2019; Sagan *et al*., 2020). Several studies have developed a moderately robust and rigorous empirical method for SPM estimation, which is based on a single red band (Sahoo *et al*., 2022; Wirasatriya *et al*., 2023). The performance of this algorithm has also been demonstrated for the Multispectral Instrument (MSI) of Sentinel-2A/B, Moderate Resolution Imaging Spectroradiometer (MODIS), and Operational Land Imager (OLI/Landsat).

Landsat 9 continues the development of Landsat 8, carrying sensors quantized to 14 bits, which improves the signal-to-noise ratio. This enhancement will provide higher sensitivity over water bodies (Niroumand *et al*., 2022). The improvement of radiometric performance is conducted to solve problems such as stray light invasion (Masek *et al*., 2020). This research offers a filtering technique that combines the entire Landsat band with the 15-m resolution panchromatic band to achieve the best atmospheric correction and image enhancement. Previous studies using Landsat 8 imagery have been conducted in BKT Semarang and its surroundings by Subiyanto (2017) and Febrianto and Latifah (2017). However, these studies lack a validation test based on field data, and the model was not built based on data acquisition taken simultaneously for using algorithms derived from other waters with varying optical properties. In complex water, such as coastal areas, a qualitative approach to suspected particle suspensions can be estimated using algorithms developed in other water areas. However, field data still need to validate these algorithms (Long, 2013). This research aims to develop a precise algorithm to predict SPM concentrations in Semarang waters spatially and temporally, especially near the mouth of the BKT, and to evaluate the correlation of hydro-oceanographic parameters, including precipitation, wind speed, and tides in triggering the variability of SPM.

Materials and Methods

This study was conducted in the Banjir Kanal Timur Estuary, Semarang City, Central Java, Indonesia, between 110.43-110.46° East and 6.9-6.96° South. We determined 100 sample points in the study area based on the transect sampling method. Samples were taken beneath less than 1-m depth, and the distance between stations is 200 m. Stations 1–50 were selected as typical references for the estuary-affected water bodies. The odd-numbered stations (1,3,5,7..,99) are used for algorithm tuning, and the even-numbered stations (2,4,6,..,100) are used for model validation (Figure 1.).

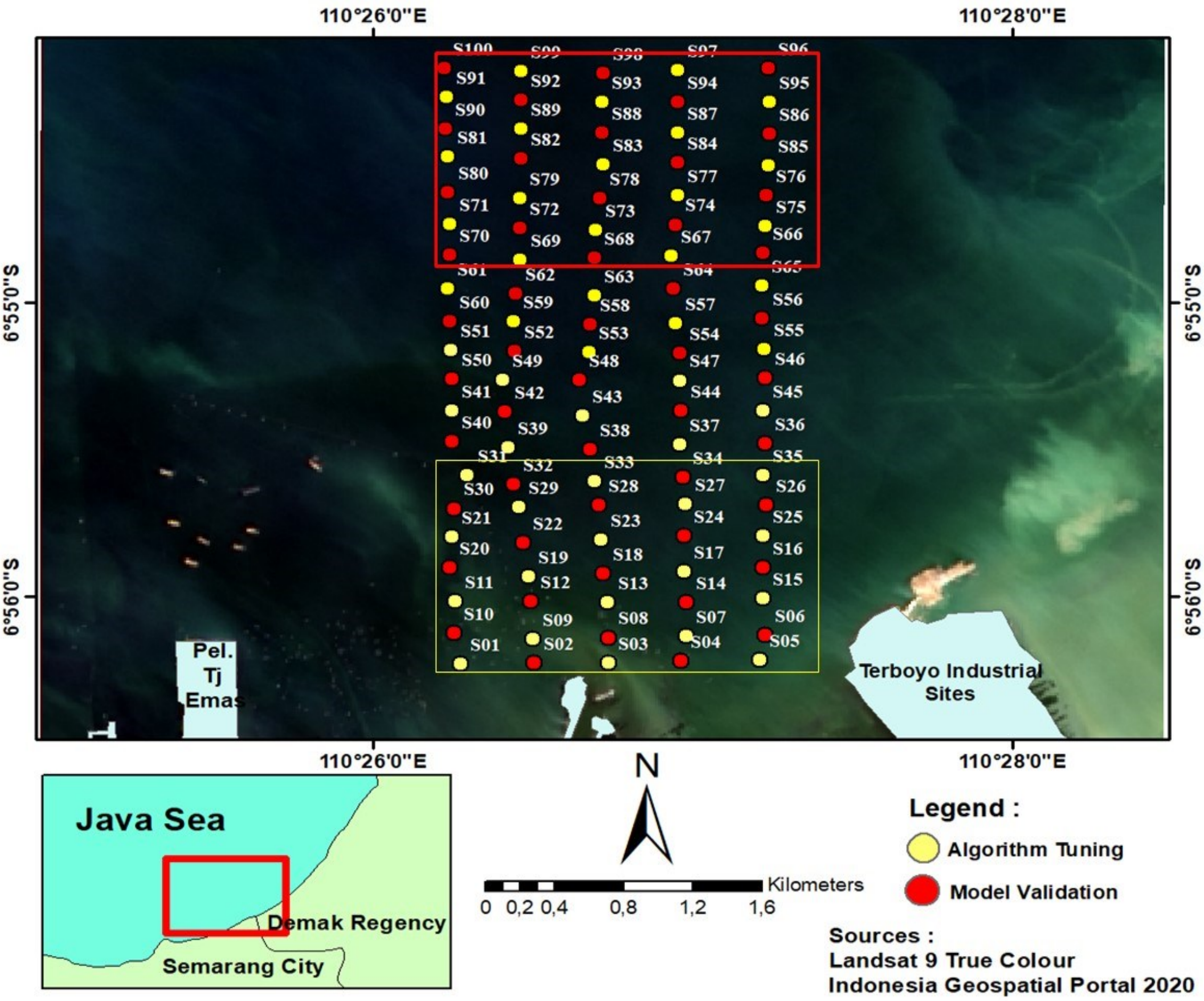

Figure 1. Research location (yellow box (area inshore), red box, area offshore)

Field sampling and analysis

The polyethylene sample bottles were used as containers for water samples. On the other hand, since we applied image processing data as the secondary data, the primary data collection should be adjusted to the satellite's passing time. Water quality sampling was carried out at 09.15-12.30 WIB (Western Indonesia Time). This time is assumed to be within the passing time range of the Landsat 9 satellite at 10.15 WIB.

The SPM analysis was carried out using a gravimetric method by weighing a purposed substance separated from other substances after filtration (Marpaung and Romelan, 2018). The filtration process was done using a vacuum pump. The SPM concentration value was calculated using the formula as follows:

$$\boldsymbol{SPM} = \frac{(\boldsymbol{a}-\boldsymbol{b})}{\boldsymbol{c}}(\boldsymbol{mg}.\boldsymbol{L}^{-1})$$

where “a” is the weight of the filtered filter paper (g), “b” is the weight of the initial filter paper (g), and “c” is the volume of filtered water, TSS concentration in $mg.L^{-1}$ (APHA, 2012).

The acquisition and processing of remote sensing imagery

The Landsat Level 1 imagery used has been geometrically corrected to improve the coordinates of the data to match the actual location on the earth's surface (USGS, 2021). The study’s Landsat image processing steps follow LAPAN (2015), which consist of: (1) Radiometric correction, which is a stage of image enhancement due to shifts in the value of optical system defects due to interference from electromagnetic radiation in the environment, (2) Image sharpening with resampling (nearest neighbour) and spatial filtering with the Gram-Schmidt sharp 5x5 method, (3) Atmospheric correction by finding the minimum pixel value, thus showing that the image is not affected by the influence of water vapour, ozone and aerosols until the reflectance at Bottom of Atmosfer (BOA). The reflectance of BOA and in situ TSS data were tested using regression analysis to derive the algorithm. The highest coefficient of determination (R^2) value indicates the best performance of an algorithm, which will then be validated. From the selected algorithm, a band math feature was created on the temporal acquisition image.

Validation models

The SPM estimation algorithm model in this study requires the input of multiple reflectances from Landsat bands, which increased the uncertainty of the estimation results. Da Silva *et al*. (2015) explained that the study of a model needs to be validate and its accuracy needs to be tested with in-situ data. Validation in this study is a statistical process that helps to determine the comparison of the algorithm equations obtained through linear, exponential, logarithmic, and polynomial regression approaches against the selected algorithm band combinations. In this study, we tested the performance of the algorithms as conducted by Balasubramanian *et al.* (2020) by calculating the root mean square error (RMSE), mean absolute perception error (MAPE), and bias value with equations 1, 2, and 3 as follows:

$$RMSE = \sqrt{\frac{1}{n}\left(x_{obs} - x_{pre}\right)^2} \quad (1)$$

$$Bias = (SPM_{pre} - SPM_{obs}) \quad (2)$$

$$MAPE = (\frac{1}{n})\sum_{i=1}^{n}\left|\frac{x_{pre}-x_{obs}}{x_{pre}}\right| \times 100\% \quad (3)$$

Meteorological and tidal data

There are various parameters that affect SPM concentrations, including surface currents (wind speed and direction), precipitation, and tides. These data were obtained through the data provider website presented in Table 1.

Result and Discussion

Suspended Particulate Matter (SPM) is one of the parameters that determine water quality (Niroumand-Jadidi *et al*., 2022). Its presence in the water column is non-toxic, but excessive concentrations can increase turbidity and reduce sunlight penetration into the water column, further

Table 1. Data Sources of Hydro-oceanographic Parameters

No.	Parameters	Source
1	Wind Speed	https://dataonline.bmkg.go.id/
2	Precipitation	https://data.chc.ucsb.edu/
3	Daily Tidal Elevation	http://ina-sealevelmonitoring.big.go.id/

impacts are inhibited photosynthesis, low dissolved oxygen, and the affected respiration of fish (Wang *et al*., 2017; Patel *et al.*, 2022). Monitoring the presence of SPM in waters must be continuous. One method that can be used to determine its concentration is the remote sensing method. This study used Landsat 9 which has a spatial resolution of 60m, since it is in a narrow area, namely at the scale of the coastal area in front of an estuary. Previous research by Febrianto and Latifah (2017) in the waters of BKT and its surroundings was not validated against in-situ data, so its accuracy is unknown. Likewise, Subiyanto (2017) directly applied algorithms from other waters that were not necessarily appropriate. Another key to success is using reflectance data that matches the optical properties reflected by the surface of the water.

The accuracy of the atmospheric correction will determine the reflectance value and affect the estimated TSS value (Zhang *et al*., 2010; Jaelani *et al*., 2015). Atmospheric conditions can affect electromagnetic radiation from the sun to the object and from the object to the sensor, resulting in differences in reflectance values. There are two types of reflectance values, namely Top of Atmosphere (ToA) and Bottom of Atmosphere (BoA). ToA reflectance is the reflectance that the sensor captures, resulting from radiometric calibration. BoA reflectance is generated from atmospheric correction processes, such as the Dark Object Subtraction (DOS), and Fast Line of Sight Atmospheric Analysis of Spectral Hypercubes (FLAASH) methods. In this study, we have simulated several filtering methods and the atmospheric correction method with DOS shows better than the other two filtering methods (Figure 1). The results of Novitasari *et al*. (2020) found that atmospheric correction using the DOS method in determining SPM in BKT waters showed a better relationship than FLAASH and TOA reflectance. Zhang *et al*. (2010) and Cui *et al.* (2017) also showed that the DOS method produced better atmospheric correction results.

Generate SPM algorithm

Laili *et al*. (2015) explained that water quality information (*i.e.* SPM) from imagery using algorithms that have been degenerated and developed from other waters still get less accurate values. Adjovu *et al.* (2023) explain that the SPM is an optically active parameter. The dynamic changes and specific characteristics of each area make it necessary to evaluate and validate in other waters of the region. The optical properties of the coastal water column are very complex because it consists of organic (living organisms and detritus) and inorganic (sediment/non-algae) materials. This causes the relationship between SPM and reflectance at each wavelength to be highly nonlinear. A coastal water dominated by algae will produce different optical properties from an abraded or eroded coastal water with high inorganic sediments. Likewise, the type of algae that can live in each water body varies greatly (green, brown, red, *etc.*), which will certainly affect the optical properties of the water body. Runyan *et al.* (2020) explained that particle size, shape, and colour of water will affect the resulting optical properties. This optical complexity is the cause of the difficulty in generating a universal algorithm for SPM estimation. In addition, the geomorphology of the coastal area, river inputs, and local coastal circulation affect the SPM. The application of algorithms from other regions is often not suitable. Therefore, the SPM estimation becomes inaccurate and requires an improved algorithm (Pitchaikani *et al*., 2019).

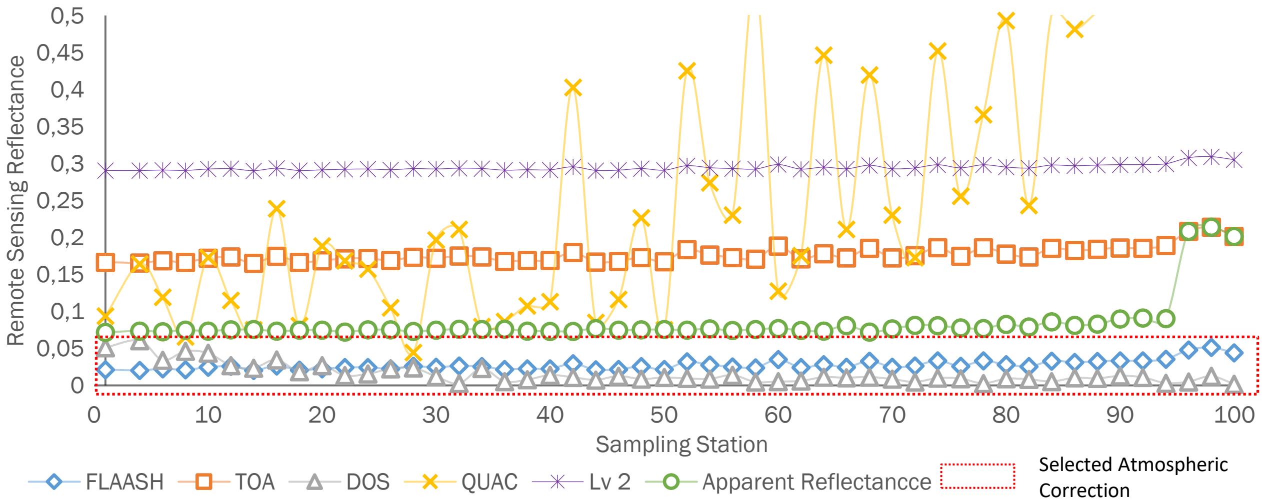

Figure 2. Reflectance variation in area study

Furthermore, from the selected reflectance data, we generated an-empirical algorithm based on the statistical relationship between the in-situ SPM and the selected Rrs, to estimate the SPM from spectral reflectance. In this study, we also simulated the use of algorithms based on a single (red) band and a combination of blue and red bands using in-situ SPM data as done by Parwati (2014), Wirasatriya *et al*. (2023) and Lailli *et al.* (2014) generated from Indonesian waters, but the coefficient of determination did not show the strongest value (Table 2). These results indicate that the best wavelength bands for estimating SPM in this study are 0.433-0.453 nm, 0.450-0.515 nm, and 0.525-0.600 nm which are the wavelengths of coastal/aerosol, blue and green respectively. The algorithm obtained in this study is still better than that developed by Adawiah *et al*. (2021) in Bekasi coast waters, with an RMSE value of >100 mg.L^{-1}. This is thought to be due to the reflectance value used without using the filtering method and the algorithm used is based on a single band. The results of research by Jaelani *et al*. (2016) also show that with the combination of band 2 and band 3, the resulting algorithm has a coefficient of determination (R^2) value below 0.5. The study by Zhao *et al*. (2020) in the China Reservoir obtained a value of RMSE=6.24 mg.L^{-1}, MAPE=18.02% (N=15) with a ranges value of 12.55-31.54 mg.L^{-1}. This SPM estimate was generated through three bands: B1, B2 and B3. The simulation of the band 1 combination algorithm with band 4 has been carried out by Laili *et al.* (2015) by producing an R^2 value >0.5. The use of a combination of band 1 with other bands has previously been carried out by Islam *et al.* (2004), Lathrop *et al.* (1991), and Ritchie *et al.* (1991).

Validation of the SPM prediction

By implementing the best algorithm generated on the Landsat 9 image (Formula 4.), the estimated SPM values in front of the BKT estuary ranged from 37.138 to 70.141 mg.L^{-1}. The scatter plot between the estimated and in-situ values is shown in Figure 3, with the bias, RMSE, and MAPE values obtained being 0.280, 5.551 mg.L^{-1}, and 7.072%. These are superior to the estimation generated by Wirasatriya *et al*. (2023) in front of the BKB estuary, Semarang (±2 km away from the study site) using Sentinel 2 imagery and a single red band algorithm. This indicates that the predicted SPM of the BKT river estimated from the algorithm can fairly well describe the observed SPM.

Table 2. Analysis of Algorithm Model for TSS Estimation from Landsat-9 images (The highest coefficient of determination is shown in bold)

Single Band/Combination Band	Statistical test				Single Band/Combination Band	Statistical test			
	Model	Verification				Model	Verification		
	R^2	RMSE	MAPE	Bias		R^2	RMSE	MAPE	Bias
B1	0.393	11.931	12.023	3.21	B4-B2	0.504	10.929	10.455	2.858
B2	0.378	10.045	11.168	2.911	B1-B3	0.522	8.544	10.579	2.304
B3	0.438	8.37	10.943	2.116	B2+B4	0.453	9.655	12.262	2.387
B4 (Parwati, 2014)	0.495	10.669	13.028	3.155	B2*B3	0.491	9.619	12.096	2.636
B5	0.456	9.706	11.061	2.067	B5/B4	0.4	11.26	15.021	8.053
B2/B4 (Laili *et al.*, 2015)	0.619	6.851	8.937	0.884	B2 / B1+B3	0.677	5.551	7.072	0.28
B2/B3 (Budiman *et al.*, 2004)	0.53	7.148	9.805	1.128	(B2-B4)/ B3	0.563	7.259	9.639	1.886
B3/B2	0.616	7.065	9.649	1.561	B1*B3 / B3*B4	0.501	7.211	10.055	1.78
B4/B2	0.56	8.57	11.256	2.409	B3*B4 / B2*B5	0.554	7.014	10.496	4.209
B1/B4	0.628	7.079	9.307	1.415	B3+B4 / B2/B4	0.549	8.39	10.674	2.035
B4/B1	0.435	10.623	10.623	1.945	B3+B4 / B3/B4	0.572	7.759	13.438	3.397
B3/B1	0.565	7.961	10.582	1.947	B2, B3, B4	0.46	10.835	16.446	2.508
B3+B4	0.591	7.764	12.041	2.591	B3, B4, B5	0.506	8.109	13.588	2.486
B2 / B3+B4	0.571	7.124	9.4	0.889	B1,B2,B3,B4,B5	0.344	14.068	19.165	7.551
B3-B2	0.571	8.012	9.991	2.164	B2,B3,B4,B5	0.537	7.21	10.238	1.573

Spatial-Temporal distribution of Suspended Particulate Matter (SPM)

The generated and validated algorithm was then applied temporally and spatially using Landsat 9 images. The dark blue color was used to represent the distribution with a range of slightly fewer values and moving into the red color which shows the higher values (Figure 4.).

The monthly fluctuations pattern is related to the precipitation. The amount of precipitation in Indonesia is strongly related to the season. The BKT estuary, Semarang-Indonesia is part of the North Sea of Java, which is influenced by the Asian and Australian monsoons. From December - February the rainy season occurs and from June to August, the summer season takes place (Alifdini *et al*., 2021). The first and second transitional seasons occur from March to May (from September to November), respectively. The monthly fluctuations of SPM in 2021-2022 of the BKT River are depicted in Figure 5. In February 2022 (February 17, 2022) the graphic shows a very high level. The influence of tidal currents contributes to the distribution pattern and fluctuation of SPM (Hutasuhut *et al*., 2022). This is shown in Figure 6

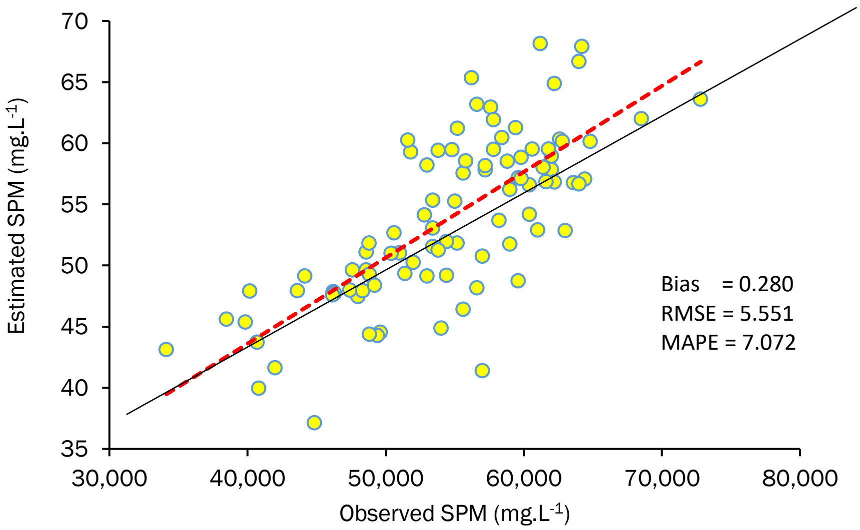

Figure 3. Validation of estimated SPM prediction with the SPM observed (in-situ data)

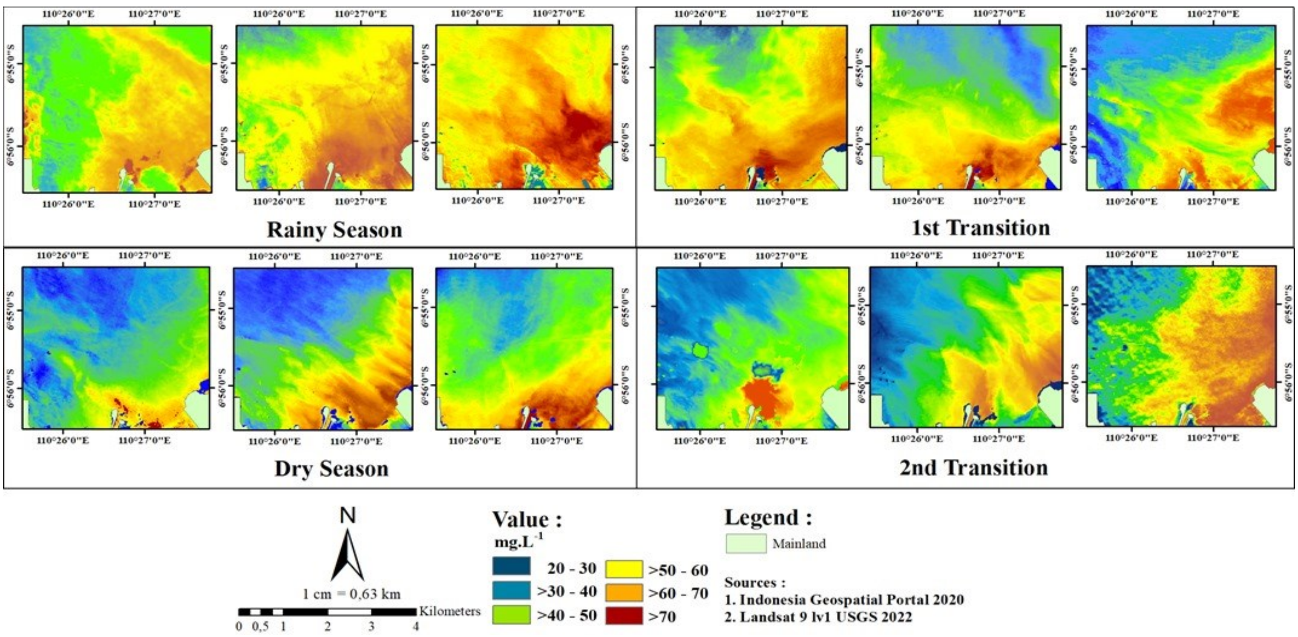

Figure 4. Suspended Particulate Matter (SPM) distributions estimated from Landsat imagery (December 2021 – November 2022) with the best algorithm (Formula 4.)

Figure 6 (boxes A and B) as evidence of higher SPM in February and lower SPM in June due to tidal conditions. The February spatial distribution pattern (Figure 4) also shows that a high SPM plume of more than 70 mg.L^{-1} was observed in front of the BKT river channel. In February, this high SPM plume extended even further and combined with the high SPM from the estuary. In contrast, the SPM fluctuation pattern in the dry season was observed to be the lowest and the SPM plume showed a narrower area, which was shown to be the lowest in the BKT estuary in June (June 25, 2022). This shows the dominating influence of the BKB River's involvement as a sediment source. River discharge is a major contributor that carries sediment to estuarine and coastal waters, thus influencing the pattern of variation in suspended sediment concentrations in the water (Pitchaikan *et al*., 2018; Zhao *et al*, 2020; Cai *et al*., 2022; Patel *et al*., 2022). The process of turbulence and tidal currents that cause sediment to remain drifting in the water column occurs simultaneously. During the rainy season, the river discharge is high and this is the most important factor in increasing the concentration of suspense sediment in the estuarine waters. In addition to tides, wave action also affects the level of turbidity in estuarine areas. Wave action in Indonesian waters is strongly related to high wind speeds (Sugianto *et al*., 2017).

Further analysis of the spatial pattern in this study we divided two areas, namely, nearshore and offshore. Figure 5 shows the same pattern of fluctuation, except for a slightly different one in February, where the offshore does not show a high. This is due to the dominant influence of the river's role as a sediment source, which in this study is closely related to precipitation. In addition, there are low tide conditions and high tides that occur, as shown in city A (Figure 6.). Wirasatriya *et al*. (2023) explained that the nearshore area (nearshore) fluctuation pattern is influenced by precipitation from the mainland. Kim *et al*. (2015) explained that precipitation is a factor that represents the high SPM from land, which causes river runoff to be high by carrying suspended material. The high wind speed is one of the triggers for currents and waves that can transport suspense sediments in coastal waters (Leclaire and Ting, 2017).

The results of statistical analysis showed that the correlation between SPM concentrations was equally strong between nearshore and offshore locations, although nearshore locations showed slightly higher SPM concentrations (Table 5.). The same pattern was found in Wirasatriya *et al*. (2023), even though this study showed a stronger correlation. A strong correlation (r=0.666) was also found between SPM fluctuations and wind speed. The nearshore location showed a stronger positive significance than the location of the estuary. This indicates the role of wind, which causes sediment resuspension, increasing the concentration of suspense sediment in the water column and transporting suspense from the estuary. Resuspension is an important source of SPM in waters (Wirasatriya *et al*., 2023).

The correlation between precipitation and SPM is r=0.924 nearshore and r=0.832 offshore. Zhao *et al*. (2020) explained that the wet season is the cause of high SPM in water bodies, but not always, due to the high anthropogenic activities that cause high SPM in the dry season. The other parameter that can cause high SPM is wind speed. The wind speed that affects the movement of surface currents for the results of

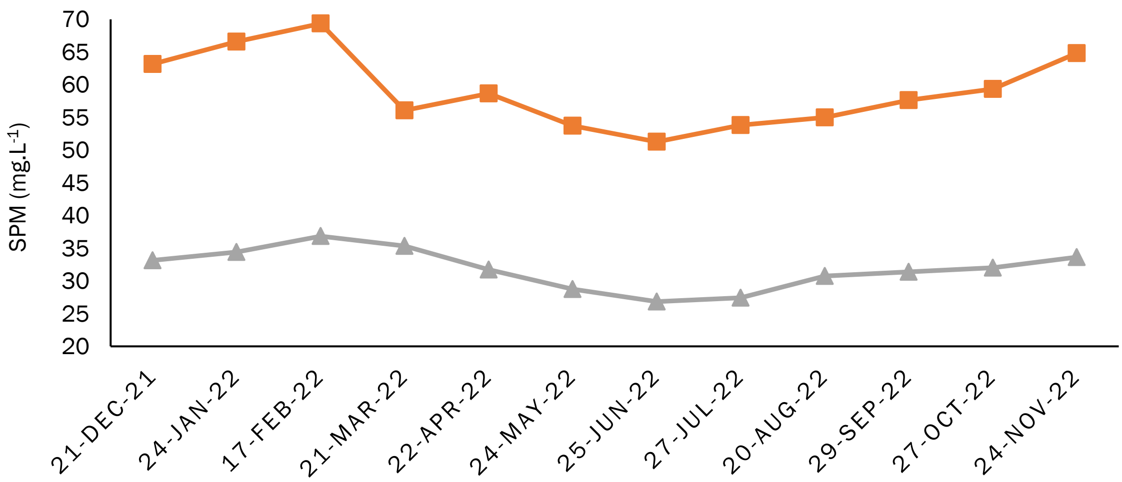

Figure 5. Temporal variation of SPM from nearshore and offshore (December 2021-November 2022)

the relationship with TSS obtained a correlation coefficient of r= 0.666 nearshore and r= 0.518 offshore. The influence of tidal fluctuations can be seen with the correlation value at TSS is r= -0.676 in nearshore and r= -0.668 offshore. A positive coefficient indicates a unidirectional relationship while a negative coefficient indicates an opposite relationship. The apparent result can be seen in Table 5.

In this study, the influence of the sea-sourced factor is represented by wind speed, where the bathymetry of the BKT estuary is relatively shallow. An increase in wind speed causes the rate of mixing water masses from the surface bottom. Wind characteristics at the acquisition time of satellite imagery showed suitability to the west monsoon season that occurred in December-February, which indicated more robust winds with a direction of 285-299 degrees, defined by cardinal directions that defined west-northwest direction. This season's condition matches with Alifdini *et al*. (2021) that the situation of Java Sea (including the coastal area of Semarang) during the rainy season is dominated by northwest wind direction with high speed, while during the dry season dominated by east to southeast wind direction with lower wind speed as shown in Figure 7.

The tidal correlation in Table 5 defines the influence of fluctuations on TSS values. The results of Figure 6 show that the sea level in the rainy season was acquired in the condition of high tide to low tide elevation alongside the increase of TSS value. While during the east season, the sea level is set from the flood tides toward the ebb, followed by a decrease in TSS value.

The relationship between each parameter was also visualized using principal components analysis by performing a linear transformation but maintaining the variance of the data to make it easier to interpret the data without significantly reducing the characteristics of the data. The results of the analysis are shown in Figure 8.

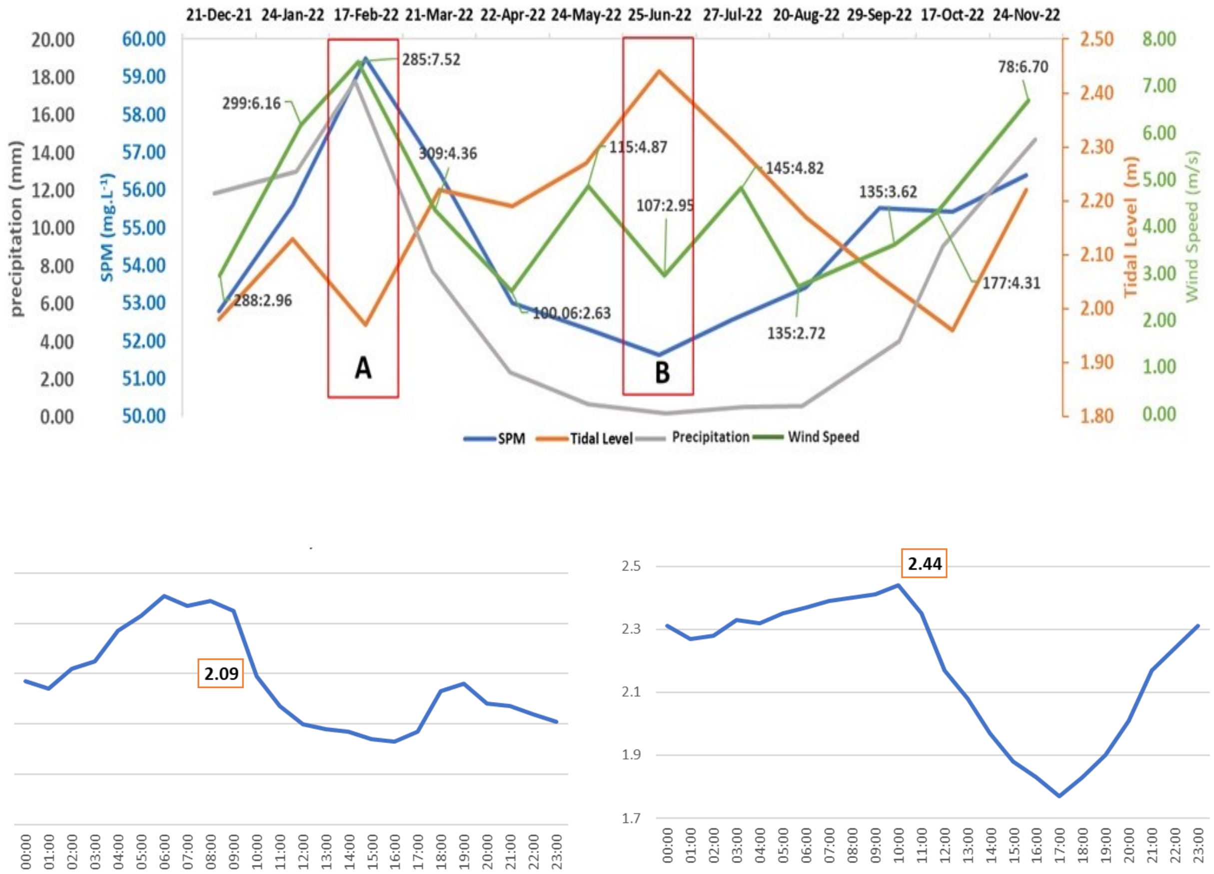

a. 17 February 2022

b. 25 June 2022

Figure 6. Time series of precipitation, wind speed, tidal fluctuations and SPM

Table 5. Correlation SPM with precipitation, wind speed and tidal level in nearshore and offshore

		Precipitation	Wind Speed	Tidal Level
Nearshore SPM	Pearson Correlation	.924**	.666*	-.676*
	Sig. (2-tailed)	.000	.018	.016
Offshore SPM	Pearson Correlation	.832**	.518	-.668*
	Sig. (2-tailed)	.001	.084	.018

*. Correlation is significant at the 0.05 level (2-tailed).
**. Correlation is significant at the 0.01 level (2-tailed).

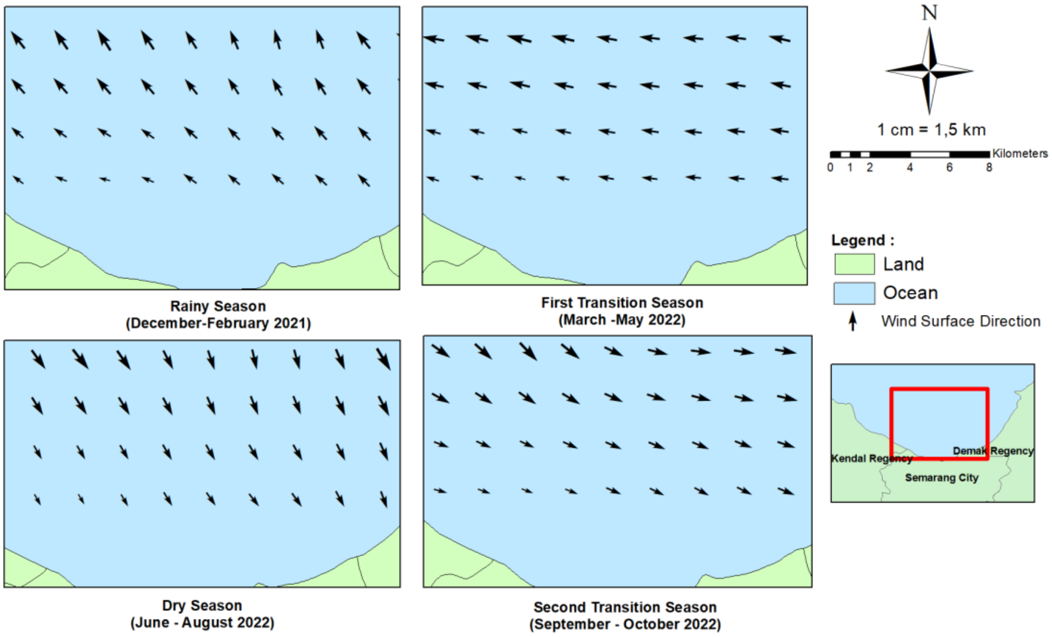

Figure 7. Wind direction in off shore coastal water of Semarang B

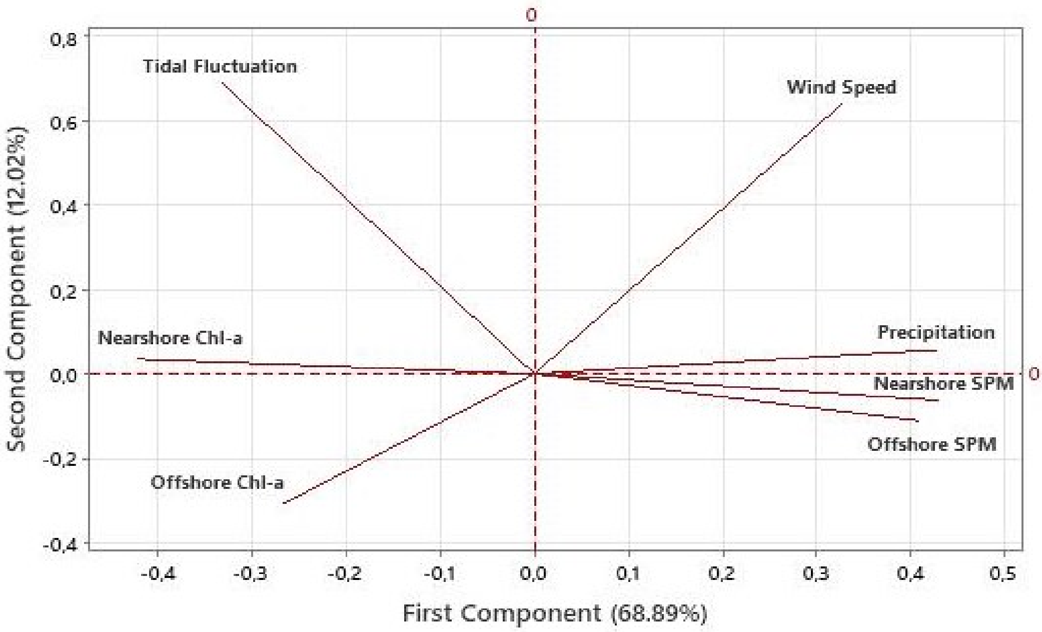

Figure 8. Principal Component Analysis of TSS with Hydro-Oceanographic Factors

Overall data homogeneity obtained was 80.91%. According to Jolliffe and Cadima (2016), the results of the principal component analysis provide important information that describes the relationship between parameters centered on the main component. The results show that TSS in nearshore and offshore have a strong positive correlation. This illustrates how the wind, interpretation, and tides parameters affect the distribution of TSS concentration value.

Conclusion

The reflectance values resulting from BoA filtering show better performances using DOS compared to FLAASH. The best performing algorithm resulted from the comparison of B2 to B1 and B3 with the formula: [SPM(mg.L^{-1})] = 164.86 x ($\frac{B2}{B1+B3}$) - 32.732, which has a coefficient of determination R^2 = 0.68, MAPE = 7.07%, bias = 0.28 mg.L^{-1}, and RMSE = 5.55 mg.L^{-1}. The resulting SPM prediction values ranged from 37.138 to 70.141 mg.L^{-1}. The temporal fluctuations of the SPM values were influenced by rainfall and water level fluctuations as well as wind. In this study, it is important to note that this algorithm was generated only during the summer season. By developing an algorithm using data that covers the dry and rainy seasons, this method can be utilized for mapping the pollution index of Semarang's eutrophic coastal waters spatially and temporally. In addition, the results obtained from this work can be beneficially utilized by regional and local authorities to better manage coastal water quality (through the creation of reservoirs) and monitoring systems.

Acknowledgment

This work was supported by Diponegoro University (RPI Scheme, No.609-60/UN7.D2/PP/VIII /2023) with the title "Algorithmic Model for Determining Suspended Particulate and Chlorophyll-a Based on Landsat Imagery for Monitoring Environmental Degradation of Coastal Waters of Semarang".

References

Adawiah, S.W., Setiawan, K.T., Parwati, E. & Faristyawan, R. 2021. Development of Empirical Model of Total Suspended Solid (TSS) by using Landsat 8 on the Coast of Bekasi Regency. *IOP Conf. Series: Earth Environ. Sci.,* 750(1): p.012039. https://doi.org/10.1088/1755-13 15/750/1/012039.

Adjovu, G.E., Stephen. H., James, D. & Ahmad, S. 2023. Measurement of Total Dissolved Solids and Total Suspended Solids in Water Systems: A Review of the Issues, Conventional, and Remote Sensing Techniques. *Remote Sens.*, 15(14): p.3534. https://doi.org/10.3390/rs15143534.

Alifdini, I., Shimada, T. & Wirasatriya, A., 2021. Seasonal distribution and variability of surface winds in the Indonesian seas using scatterometer and reanalysis data. *Int. J. Climatol.* 41 (10): 4825–4843. https://doi.org/ 10. 1002/joc.7101.

APHA [American Public Health Association]. 2012. Standards methods for the examination of water and wastewater, 22nd Edition. Washington D.C.: American Public Health Association.

Balasubramanian, S.V., Pahlevan, N., Smith, B., Binding, C., Schalles, J., Loisel, H., Gurlin, D., Greb, S., Alikas, K., Randla, Bunkei, M., Moses, W., Nguyễnm, H., Lehmann, M.K., O'Donnell, D., Ondrusek, M., Han, T.H., Fichot, C.G., Moore, T. & Boss, E. 2020. A robust algorithm for estimating total suspended solids (TSS) in inland and nearshore coastal waters. *Remote Sens. Environ.,* 246: p.111768. https://doi.org/10.10 16/j.rse.2020.111768.

Bernardo, N., Carmo, A. D., Park, E. & Alcântara, E. 2019. Retrieval of suspended particulate matter in inland waters with widely differing optical properties using a semi-analytical scheme. *Remote Sens.,* 11(19): p.2283. https://doi.org/ 10.3390/rs11192283.

Budhiman, S., Hobma, T.W. & Vekerdy, Z. 2004. Remote sensing for mapping TSM concentration in Mahakam Delta: an analytical approach. In: Liu *et al*. (eds.). Proceeding of The Thirteen OMISAR Workshop on Validation and Application of Satellite Data for Marine Resources Conservation 2004, Bali, October 5-9 2004. 1-15 pp.

Cai, L., Chen, S., Yan, X., Bai, Y. & Bu, J. 2022. Study on High-Resolution Suspended Sediment Distribution under the Influence of Coastal Zone Engineering in the Yangtze River Mouth, China. *Remote Sens.,* 14: p.486. https://doi.org/10. 3390/ rs14030486

Colella, S., Falcini, F., Rinaldi, E., Sammartino, M. & Santoleri, R. 2016. Mediterranean ocean color chlorophyll trends. *PLoS ONE,* 11(6): e0155756. https://doi.org/10.1371/journal.pone.0155756

Cui, L., Li, G., Ren, H., He, L., Liao, H., Ouyang, N. & Zhang, Y. 2017. Assessment of atmospheric correction methods for historical Landsat TM images in the coastal zone: A case study in

Jiangsu, China. *Eur. J. Remote Sens.,* 47: 701-716. https://doi.org/10.5721/EuJRS20144740

Doxaran, D., Ehn, J., Bélanger, S., Matsuoka, A., Hooker, S. & Babin, M. 2012. Optical characterisation of suspended particles in the Mackenzie River plume (Canadian Arctic Ocean) and implications for ocean colour remote sensing. *Biogeosciences,* 9: 3213-3229

Febrianto, S. & Latifah, N. 2017. Mapping the Distribution Pattern of Total Suspended Solid (TSS) in Semarang Bay Waters Using Landsat 7 Etm and Landsat 8 Satellite Imagery. *J. Harpodon Borneo*, 10(1) :56-60 (In Bahasa)

Feng, L., Hu, C., Chen, X. & Song, Q. 2014. Influence of the Three Gorges Dam on total suspended matters in the Yangtze estuary and its adjacent coastal waters: observations from MODIS. *Remote Sens. Environ.,* 140: 779–788.

Gordon, H. R. & Wang, M. 1994. Retrieval of water-leaving radiance and aerosol optical thickness over the oceans with SeaWiFS: A preliminary algorithm. *Applied Optics,* 33(3): 443–452

Irwansyah, I., Isma, F., Ismida, Y., Isma, M. F., Sufahani, S.F. & Akbar, H. 2023. Effect of Stream River and Tidal on the Suspended Sediment Concentration of Kuala Langsa Estuary, Aceh, Indonesia. *Ilmu Kelautan: Indonesian Journal of Marine Sciences*, 28(1): 27-36, https://doi.org/10.14710/ik.ijms.28.1.27-36.

Islam, S., Sarker, J. Yamamoto, T., Wahab, A. & Tanaka, M. 2004. Water and sediment quality, partial mass budget, and effluent N loading in coastal brackishwater shrimp farms in Bangladesh. *Mar. Poll. Bull.,* 48: 471–485.

Jaelani, L.M., Matsushita, B., Yang, W. & Fukushima, T. 2015. An improved atmospheric correction algorithm for applying MERIS data to very turbid inland waters. *Int. J. Appl. Earth Obs. Geoinf.,* 39: 128–141. http://doi.org/10.1016/j.jag.2015.03.004.

Jaelani, L.M., Limehuwey, R., Kurniadin, N., Pamungkas, A., Koenhardono, E.S. & Sulisetyono, A. 2016. Estimation of Total Suspended Sediment and Chlorophyll-A Concentration from Landsat 8-Oli: The Effect of Atmosphere and Retrieval Algorithm. *IPTEK The J. Technol. Sci.*, 27(1): 16-23. https://doi.org/10.12962/j20882033.v27 i1.1217

Jolliffe, I.T. & Cadima, J. 2016. Principal component analysis: a review and recent developments. *Philos. Trans. A Math. Phys. Eng. Sci.*, 374(2065): p.20150202. https://doi.org/10.1098/rsta.20 15.0202.

Kim, Y. H., Im, J., Ha, H. K., Choi, J.K. & Ha, S. 2014. Machine Learning Approaches to Coastal Water Quality Monitoring Using GOCI Satellite Data. *GIScience & Remote Sens.,* 51: 158-174, https://doi.org/10.1080/15481603.2014.900983.

Laili, N., Arafah, F., Jaelani, L.M., Subehi, L., Pamungkas, A., Koenhardono, E.S. & Sulisetyono, A. 2015. development of water quality parameter retrieval algorithms for estimating total suspended solids and chlorophyll-a concentration using Landsat-8 imagery at Poteran Island Water. *ISPRS Annals of the Photogrammetry, Remote Sensing and Spatial Information Sciences,* II-2/W2: 55-62. https://doi.org/10.5194/isprsannals-II-2-W2-55-2015.

LAPAN. 2015. Pedoman Pemanfaatan Data Landsat 8 untuk Deteksi Daerah Terbakar (Burned Area). Jakarta: Pusfatja Lapan

Lathrop, R.G., Lillesand, T.M. & Yandell, B.S. 1991. Testing the utility of simple multi-date Thematic Mapper calibration algorithms for monitoring turbid inland waters. *Remote Sens*.,12: 2045–2063

LeClaire, P.D. & Ting, F.C.K. 2017. Measurements of suspended sediment transport and turbulent coherent structures induced by breaking waves using two-phase volumetric three-component velocimetry. *Coast. Eng.,* 121: 56–76, https://doi.org/10.1016/j.coastaleng.2016.11.008

Long, C.M. & Pavelsky, T.M., 2013. Remote sensing of suspended sediment concentration and hydrologic connectivity in a complex wetland environment. *Remote Sens. Environ*., 129: 197–209.

Marpaung, M.P. & Romelan, 2018. Analisis Jenis dan Kadar Saponin Ekstrak Metanol Daun Kemangi (*Ocimum basilicum* L.) dengan Menggunakan Metode Gravimetri. *J. Farmasi Lampung*, 7(2): 81-86. https://doi.org/10.37090/jfl.v7i2. 57

Masek, J. G., Wulder, M. A., Markham, B., McCorkel, J., Crawford, C. J., Storey, J. & Jenstrom, D. T. 2020. Landsat 9:Empowering open science and applications through continuity. *Remote Sens. Environ.,* 248: p.111968. https://doi.org/10.1016/j.rse.2020.111968

Maslukah, L., Zainuri, M., Wirasatriya, A. & Maisyarah, S. 2020. The Relationship among Dissolved

Inorganic Phosphate, Particulate Inorganic Phosphate, and Chlorophyll-a in Different Seasons in the Coastal Seas of Semarang and Jepara. *J. Ecol. Eng.,* 21(3): 135–142

Mishra, S., D.R. Mishra, D.R., Lee, Z. & Tucker, C.S. 2013. Quantifying cyanobacterial phycocyanin concentration in turbid productive waters: a quasi-analytical approach. *Remote Sens. Environ.,* 133: 141-151

Nechad, B., K.G. & Ruddick, G. 2009. Neukermans Calibration and validation of a generic multisensor algorithm for mapping of turbidity in coastal waters SPIE European Int. Symp. On Remote Sens, Berlin.

Niroumand-Jadidi, M., Bovolo, F., Bresciani, M., Gege, P. & Giardino, C. 2022. Water Quality Retrieval from Landsat-9 (OLI-2) Imagery and Comparison to Sentinel-2. *Remote Sens.*, *14*(18): p.4596. https://doi.org/10.3390/rs14184596

Novitasari, N., Sukmono, A. & Bashit, N. 2020. analisa pengaruh koreksi atmosfer terhadap akurasi estimasi kandungan TSS (Total Suspended Solid) menggunakan citra Landsat 8 (Studi Kasus: Muara Banjir Kanal Timur Semarang Dan Muara Das Blorong Kabupaten Kendal), *J. Geodesi UNDIP*, 9(1): 335-343.

Ouma, Y.O., Noor, K. & Herbert, K. 2020. Modeling Reservoir Chlorophyll-a, TSS, and Turbidity Using Sentinel-2A MSI and Landsat-8 OLI Satellite Sensors with Empirical Multivariate Regression. *J. Sensors,* Article ID 8858408 p.1-21. https://doi.org/10.1155/2020/8858408

Parwati, E. 2014. Analisis Dinamika Fluktuasi TSS (Total Suspended Solid) Sepanjang Das-Muara-Laut di Perairan Berau Kalimantan Timur. *Seminar Nasional Penginderaan Jauh 2014*, p.662–670.

Patel, B., Sarangi, R.K., Prajapati, Devliya, B. & Patel, H. 2022. Development of Total Suspended Matter (TSM) Algorithm and Validation over Gujarat Coastal Water, the Northeast Arabian Sea Using In Situ Datasets. *Mar. Geod.*, 45(6): 670-687.

Pitchaikani, J.S., Ramakrishnan, R, Bhaskaran, P.K, Ilangovan, D. & Rajawat, A.S. 2019. Development of Regional Algorithm to Estimate Suspended Sediment Concentration (SSC) based on the remotely sensed reCectance and Beld observations for the Hooghly Estuary and West Bengal coastal waters; *J. Indian. Soc. Remote Sens*., 47: 177–183.

Quang, N.H., Sasaki, J., Higa, H. & Huan, N.H. 2017. Spatiotemporal Variation of Turbidity Based on Landsat 8 OLI in Cam Ranh Bay and Thuy Trieu Lagoon, Vietnam. *Water,* 9(8): p.570. https://doi.org/10.3390/w9080570

Ritchie, J.C. & Cooper, C.M. 1991. An algorithm for estimating surface suspended sediment concentrations with Landsat mss digital data. *J. Am. Water Resource Assoc*., 27: 373–379.

Runyan, H., Reynolds, R. A. & Stramski, D. 2020. Evaluation of Particle Size Distribution Metrics to Estimate the Relative Contributions of Different Size Fractions Based on Measurements in Arctic Waters. *J. Geophys. Res. Oceans,* 125: e2020JC016218. https://doi.org/10.1029/2020jc016218

Saberioona, M., Bromc, J., Nedbalc, V., Soucek̆, P. & Císar, P. 2020. Chlorophyll-a and total suspended solids retrieval and mapping using Sentinel-2A and machine learning for inland waters. *Ecol. Indic*., 113: p.106236.

Sagan, V., Peterson, T., Maimaitijiang, M., Sidike, P., Sloan, J., Greetings, B.A., Maalouf, S. & Adams, C. 2020. Monitoring inland water quality using remote sensing: potential and limitations of spectral indices, bio-optical simulations, machine learning, and cloud computing. *Earth Sci. Rev.,* 205: p.103187.

Sahoo, D.P., Sahoo, B. & Tiwari, M.K. 2022. MODIS-Landsat fusion-based single-band algorithms for TSS and turbidity estimation in an urban-waste-dominated river reach. *Water Res.,* 224: p.119082.

Shaik, I., Mohammad, S., Nagamani, P.V., Begum, S.K., Kayet, N. & Varaprasad, D. 2021. Assessment of chlorophyll-a retrieval algorithms over Kakinada and Yanam turbid coastal waters along the east coast of India using Sentinel-3A OLCI and Sentinel-2A MSI sensors. *Remote Sens. Appl.: Soc. Environ.*, 24: p.100644.

Sravanthi N., Ramana I., Yunus Ali P., Ashraf M., Ali, M. & Narayana A. 2013. An algorithm for estimating suspended sediment concentrations in the coastal waters of India using remotely sensed reflectance and its application to coastal environments. *Int. J. Environ. Res*., 7: 841–850.

Subiyanto, S. 2017. Remote sensing and water quality indicators in the west flood canal Semarang city: spatiotemporal structures of lansat-8 derived chlorophyll-a and total suspended solids. *IOP Conf. Series: Earth Environ. Sci.,* 98: 1–10.

Triadmodjo, B. 1999. Teknik Pantai. Yogyakarta: Beta Offset.

Sugianto D.N., Zainuri M., Darari A., Suripin S.D., Yuwono N. 2017. Wave height forecasting using measurement wind speed distribution equation in Java Sea, Indonesia. *Int. J. Civ. Eng. Technol.,* 8(5): 604-619

USGS. 2021. Landsat 9 Data User Handbook. USGS

Wang, Z., Kawamura, K., Sakuno, Y., Fan, X., Gong, Z. & Lim, J. 2017. Retrieval of Chlorophyll-a and Total Suspended Solids Using Iterative Stepwise Elimination Partial Least Squares (ISE-PLS) Regression Based on Field Hyperspectral Measurements in Irrigation Ponds in Higashihiro shima, Japan. *Remote Sens.,* 9(264): 1-14

Weston, N.B., 2014. Declining sediments and rising seas: an unfortunate convergence for tidal wetlands. *Estuar. Coasts* 37: 1–23

Wirasatriya, A., Maslukah, L., Indrayanti, E., Yusuf, M., Milenia., A.P., Adam, A.A. & Helmi, M. 2023. Seasonal variability of Total Suspended Sediment off the Banjir Kanal Barat River, Semarang, Indonesia estimated from Sentinel-2 images. *Reg. Stud. Mar. Sci.,* 57: p.102735.

Yu, X., Lee, Z., Shen, F., Wang, M., Wei, J., Jiang, L. & Shang, Z. 2019. An empirical algorithm to seamlessly retrieve the concentration of suspended particulate matter from water color across the ocean to turbid river mouths. *Remote Sens. Environ.,* 235: p.111491.

Zhang, M., Dong, Q., Cui, T., Xue, C. & Zhang, S. 2014. Site sediment monitoring and assessment for the Yellow River estuary was suspended from Landsat TM and ETM+ imagery. *Remote Sens. Environ.,* 146: 136-147

Zheng, G. & DiGiacomo, P.M. 2017. Uncertainties and applications of satellite-derived coastal water quality products. *Prog. Oceanogr*., 159: 45-72.

Zhang Z., He, G. & Wang, S. 2010. A practical DOS model-based atmospheric correction algorithm. *Int. J. Remote Sens*., 31(11): 2837-2852. https://doi.org/10.1080/01431160903124682

Zhao, J., Zhang, F., Chen, S., Wang, C., Chen, J., Zhou, H. & Xue, Y. 2020. Remote Sensing Evaluation of Total Suspended Solids Dynamic with Markov Model: A Case Study of Inland Reservoir across Administrative Boundary in South China. *Sensors*, 20(23): p.6911. https://doi.org/10. 3390/s2 0236911